Cytokine 113 (2019) 162–176

Contents lists available at ScienceDirect

Cytokine

journal homepage: www.elsevier.com/locate/cytokine

Antigen conjugated nanoparticles reprogrammed the tumor-conditioned macrophages toward pro-immunogenic type through regulation of NADPH oxidase and p38MAPK

Sourav Chattopadhyay[a,b], Somenath Roy[a,*]

[a] Immunology and Microbiology Laboratory, Department of Human Physiology with Community Health, Vidyasagar University, Midnapore 721 102, West Bengal, India
[b] Molecular Genetics and Therapeutics Lab, Indian Institute of Technology, Kanpur, India

ARTICLE INFO

Keywords:
Tumor conditioned macrophage
NPs-antigen
NADPH Oxidase
p38 MAPK

ABSTRACT

Tumor associated macrophages (TAMs) are pertinent to cancer cell growth in the tumor microenvironment. Indeed, TAMs differentiate from monocytes (MΦ) due to specific growth factors present in the tumor microenvironment. TAMs show mostly an M2-like phenotype is due to the absence of pro-inflammatory signals and supply fuel to tumor growth. Several attempts have been taken to switch TAMs into a pro-immunogenic type. To address context, we used a tumor microenvironment by *in vitro* coculturing human blood MΦ with cancer cell conditioned media (TC-MΦ). We showed that the antigen cobalt oxide nanoparticles (Ag-NPs) can reprogram TC-MΦ to pro-immunogenic type to build up an antitumor immune response. Our results demonstrate that NPs-Ag induced a marked activation of NADPH oxidase in TC-MΦ, likely through stimulation of ROS linked to activation of p38 MAPK. These activated p38 MAPK up-regulated the IFN-γ, TNF-α and initial IL-12 production, in turn, the activation of IFN-γ prolonged IL-12 production.

1. Introduction

Macrophages are among the first immune cells to infiltrate already preinvasive tumorous lesions and persist during the development into invasive cancer [12]. Within the tumor context, macrophages (MΦ) are increasingly recognized as pivotal regulators. Studies with the tumor microenvironment reveal that local cytokine milieu, macrophages can adopt a diverse, functional phenotype, which is often found to be opposite in nature, e.g., Inflammatory versus anti-inflammatory and tissue remodeling versus tissue destruction [18,39,38]. Once migrated to the tumor site monocytes differentiate into MΦ under the influence of macrophage colony stimulating factor (MCSF). Further tumor cell derived factors drive macrophage polarization in one of the TAM subpopulations showing the M2 phenotype [14,36], provides the fuel for cancer development and progression. Recent reports have established that the acquisition of pro-tumoral M2 functions by TAM is driven by various cytokines and signals expressed within the tumor microenvironment [40]. Among these, IL-10, PGE2, TGF-β and CSF-1 were reported to induce the M2 polarization of MΦ. Based on the M1 versus the M2 paradigm of MΦ polarization [39], inhibition of M2- and activation of M1-inducing signals was proposed as a possible strategy to restore the anti-tumor functions of TAM [3].

Nanotechnology is currently being used to engineer specific immune responses for prophylactic and therapeutic effects. Nanoparticles (NPs) are known to be able to interact with and affect the immune system. Several different types of nanoparticles have been used either alone as antigen (Ag) carriers to entrap antigens or together with other agents. A number of studies have shown that different NPs can be used to modulate immune responses against encapsulated antigens owing to their ability to proficiently target APCs (such as MΦ) and to facilitate appropriate processing and presenting of antigens [24,5,6,1,16]. Vaccine delivery vehicle composed of biodegradable polymers (PLGA) have been extensively characterized in animal models and are widely used in clinical applications as a matrix to encapsulate co-deliver and gradually release of Ags. In vaccine development, PLGA (150–200 nm in size) has been used to encapsulate hepatitis B surface antigen (HBsAg), and it promotes the rapid uptake and the endosomal localization of vaccine antigens in DCs, as well as the subsequent production of high titres of antigen-specific antibodies [25,2,31,32]. The immunomodulatory effect of NPs has also been reported previously by several scientists. The size, solubility and modified group of the NPs affect the delivery of particles to immune cells and the outcome of tumor treatments [25,2,32,31].

Previously, our *in vitro* and *in vivo* study showed that PMIDA conjugated cobalt oxide nanoparticles were successfully bound with whole

* Corresponding author.
E-mail address: sroy.vu@hotmail.com (S. Roy).

https://doi.org/10.1016/j.cyto.2018.06.035
Received 31 January 2018; Received in revised form 29 June 2018; Accepted 30 June 2018
Available online 17 July 2018

cancer lysate antigen and stimulate anticancer immune response by activating TNF-α [9,11]. We had been employ the whole tumor cell lysate as antigen in cancer immunotherapy because the recognition of the effective antigen(s) is not necessitated and treatment strategies are practicable even for such malignancies in which only few more or less specific tumor antigens have been characterized [35] and secondly, the credible presence of multiple antigens trim down the risk of a tumor cell escape. This study explain how the antigen conjugated nano sized cobalt oxide NPs escort the pro-inflammatory response via activation of ROS-NADPH oxidase depended p38 MAPK in the tumor (leukemia) conditioned MΦ. This study will help to understand the signaling mechanism triggered by the antigen conjugated NPs and maybe help to reveal the intricate relationship between the oxidative stress induced signal-transduction mechanism and alteration of the cytokine repertoire of tumor (leukemia) conditioned MΦ.

2. Methodology

2.1. Cell line cultures and tumor-conditioned media preparation

Human leukemic cancer cell lines Jurkat (IL-12$^-$/TNF-α$^+$) and KG1-A (IL-12$^-$/TNF-α$^+$) were cultured in RPMI 1640 (Sigma) supplemented with 10% FBS, 5% Co_2. Once grown to 80–90% of confluence, the media were discarded, and flasks were rinsed two times with saline solution. Cells were then incubated with fresh RPMI for 24 h; the conditioned media (CM) were collected and filtered at 0.22 μm, and the supernatant was stored at −80 °C. All cell lines were routinely checked for contamination.

2.2. Lysate antigen preparation

The homogeneous suspension of Jurkat and KG1-A cells were collected in a centrifuge tube and centrifuged at 1500 rpm for 5 min. The supernatant was pour out and the cell pellets were re-suspended in ice cold phosphate buffered saline (PBS) at concentrations ranging from 2×10^5 cells/ml and subjected to four cycles of freeze-thaw cycles (alternating liquid nitrogen and 37 °C water bath treatment) followed by sonication for 20 s (Ultrasonic Processor, Tekmar, Cincinnati, OH, USA) on ice. Lysates were centrifuged at 12,000 rpm for 20 min at 4 °C to remove cellular debris. Supernatants were collected and stored at −80 °C [30]. Protein content of lysate preparations was measured according to Lowry et al. [26] using BSA as standard.

2.2.1. Synthesis, characterization of cobalt oxide nanoparticles and conjugation with PMIDA

The cobalt oxide nanoparticles (CoO NPs) were synthesized according to our previous lab report with slight modification in temperature [11]. The prepared bulk primary structure of cobalt oxide was subjected to thermal decomposition at 800 °C to form its nano structure followed by characterization by transmission electron microscope, X-ray diffraction study. The conjugation of phosphonomethyl-immino-diacetatic acid (PMIDA) on the surface of the CoO NPs was done as per our standard lab method. Then cancer cell lysate antigen was conjugated with PMIDA-CoO NPs were technique as described in our previous paper [11].

2.3. Isolation of monocytes

Human monocytes were obtained from blood by density gradient centrifugation, using Histopaque-1077 (Sigma-Aldrich) according to our previous lab method. Remaining lymphocytes were removed from the monocytes faction by plastic adherence and all the two factions were cultured in RPMI 1640 supplemented with 10% FBS, 5% Co_2 in a Co_2 incubator.

2.4. Preparation of tumor-conditioned (TC) macrophage (MΦ)

Macrophages (MΦ) were obtained by culturing 10^6/ml monocytes for 12 days in RPMI 1640, 5% FBS supplemented. The MΦ were divided into three groups, among them one group remain untreated and other groups were cultured (10^6/ml MΦ) in RPMI 1640 5% FBS supplemented with either 30% of tumor cell line supernatants for 6 days to get tumor-conditioned macrophage (TC-MΦ) or LPS (10 ng/ml) conditioned macrophages (L-MΦ).

2.5. Macrophages pulsation with only NPs, only Ag, NP-Ag complex

All the three different groups, i.e. MΦ, TC-MΦ and L-MΦ were cultured with only NPs, only Ag, NP-Ag complex was used at a dose of 25 μg/ml, which was reported to be immunogenic [9,11] for 24 h in RPMI 1640 5% FBS. After incubation, the supernatants were collected and stored at −80 °C for further assay. The cells were collected, and suspended in fresh media.

2.6. Cytokines

Cytokine (IFN-γ, TNF-α, IL-12, IL-10) production in the supernatants of pulsed MΦ, TC-MΦ and L-MΦ were measured by specific ELISA kits (BD Biosciences) as per the manufacturers' instruction. UN-pulsed MΦ was used as negative control.

In another experimental system, MΦ, TC-MΦ and L-MΦ were treated with ROS and p38 MAPK inhibitor for 1 h. Then all the cells were pulsed with NPs-Ag complex for 24 h. After incubation, IFN-γ was estimated by using ELISA with respect to only macrophages.

2.7. ROS generation

NP-Ag complex Pulsed MΦ, TC-MΦ and L-MΦ were stained with 2,7-dichlorofluorescin diacetate (DCFH2-DA) to detect the intracellular ROS [9]. UN-pulsed MΦ was used as negative control.

2.8. Estimation of cobalt ion (Co^{++}) by atomic absorption spectroscopy (AAS)

The intracellular cobalt ion was estimated by AAS technique described as our previous paper [10].

2.9. NADPH oxidase activity

All the groups of MΦ were mixed with pre warmed in Krebs ringer buffer ((KRB) with 10 mM glucose at 37 °C for 3 min and PMA (0.1 μMol) pre-warmed at 37 °C for 5 min) then the reaction was stopped by putting in ice. Centrifugation was carried out at 400*g* for 5 min and the resultant pellet was resuspended in 0.34 M sucrose. The cells were then lysed with hypotonic lysis buffer. Centrifugation was carried out at 800*g* for 10 min and the supernatant used to determine enzyme activity. NADPH oxidase activity was determined spectrophotometrically by measuring cytochrome *c* reduction at 550 nm (Shimadzu UV-VIS-1800). The reaction mixture contained 10 mM phosphate buffer (pH 7.2), 100 mM NaCl, 1 mM $MgCl_2$, 80 μM cytochrome *c*, 2 mM sodium azide (NaN_3) and 100 μl of supernatant (final volume 1.0 ml). At last a suitable amount of NADPH (10–20 μl) was added to initiate the reaction [10].

2.10. p38 MAPK activity

Detection of p38 MAPK in the cell lysate of pulsed MΦ, TC-MΦ and L-MΦ were measured by specific ELISA kits (e Biosciences) and FACS analysis as per the manufacturers' protocol. Un-pulsed MΦ was used as negative control [41,10]. The activation of p38 MAPK was also estimated by western blotting also as per the standard methods [13] using

monoclonal mouse antibodies followed by using ALP conjugated secondary antibody and it's specific substrate NBT/BCIP to develop the blot.

2.11. Co-culture of pulsed macrophage with cancer cells

Jurkat and KG-1A cells were plated in culture plates at a density of 4×10^4 cells/well and incubated in RPMI medium with 5% FCS for 24 h at 37 °C. After 24 h, pulsed MΦ, TC-MΦ and L-MΦ were added to each well at the ratio of 5:1 or 10:1 (macrophages: cancer cells), and were then incubated for 1, 3 and 5 days at 37 °C. The cancer cell viability was estimated by crystal violet assay (0.1% V/V crystal violet was prepared in methanol). After co-culture, each well was washed with sterile saline to remove the dead macrophages (floated), Jurkat and KG-1A cells. The surviving Jurkat and KG-1A cells were stained with 0.1% crystal violet/methanol at room temperature for 10 min. The plates were read on a microplate reader (model 550, Bio-Rad, Tokyo, Japan) at a wavelength of 570 nm. Cytostasis was calculated as a percentage. The absorbance of surviving Jurkat and KG-1A cells in the absence of macrophages (control absorbance) was set at 100%, and the experimental absorbance was divided by the control absorbance.

2.12. Co-culture of NPs-Ag complex pulsed macrophage with cancer cells in the presences of ROS inhibitor, P38 MAPK inhibitor and TNF-α inhibitor

MΦ, TC-MΦ and L-MΦ were cultured 1 h in the presences or absences of NAC (ROS inhibitor) or Pyridinyl Imidazole (p38 MAPK inhibitor) [23] and POF (TNF-α inhibitor) were used at a final concentration of 5 mM, 1 mM, 2 mM respectively. After 1 h, the MΦ, TC-MΦ and L-MΦ were isolated and washed with sterile PBS for three times and cultured with NPs-Ag complex at selected dose. Jurkat and KG-1A cells were plated in culture plates at a density of 4×10^4 cells/well and

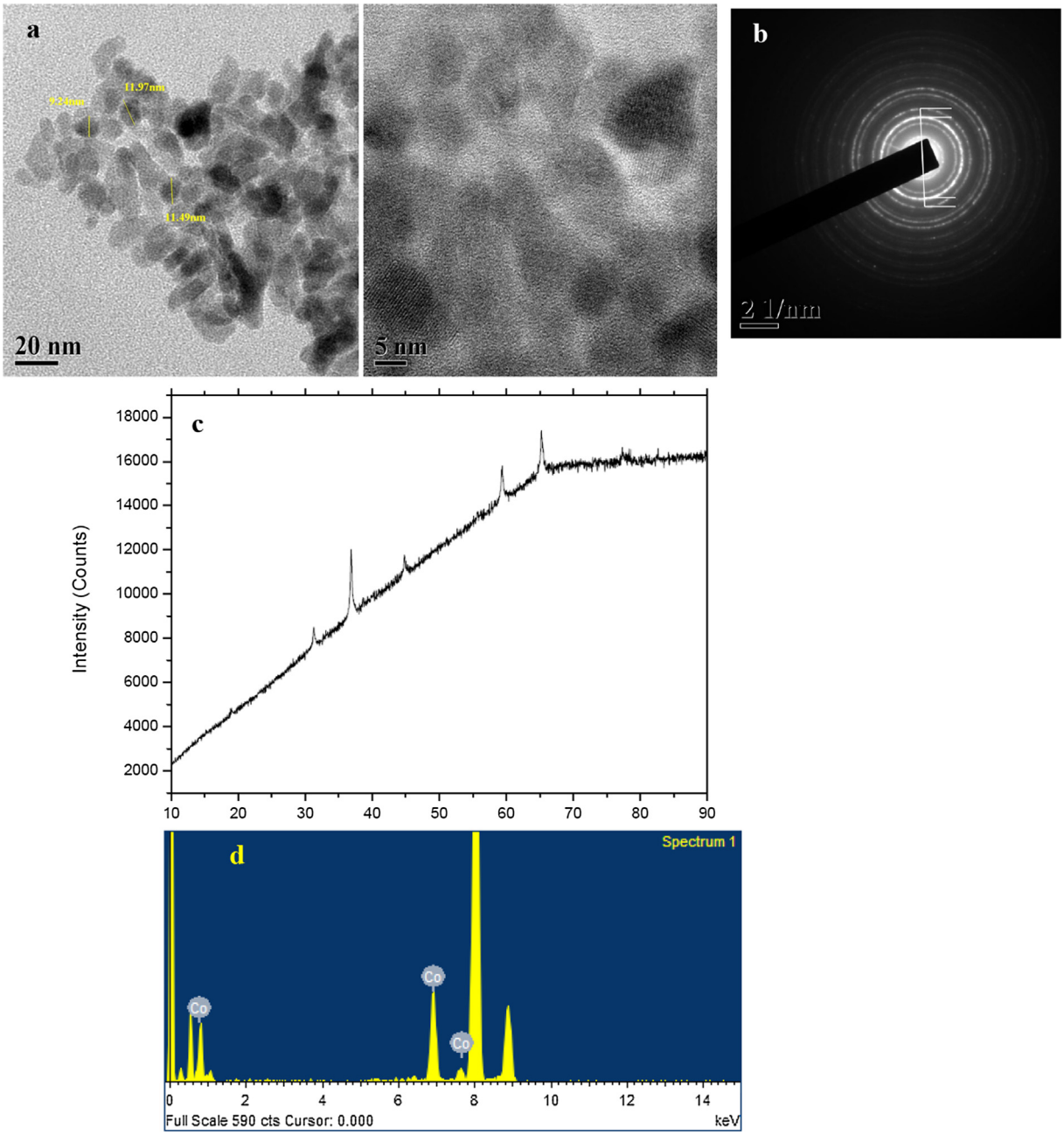

Fig. 1. TEM analysis of the synthesized cobalt oxide nanoparticles at 20 nm and 5 nm scale (a). SADE analysis of the synthesized cobalt oxide nanoparticles (b). The X-ray powder diffraction patterns of synthesized cobalt oxide nanoparticles (c). The EDX pattern of synthesized cobalt oxide nanoparticles (d).

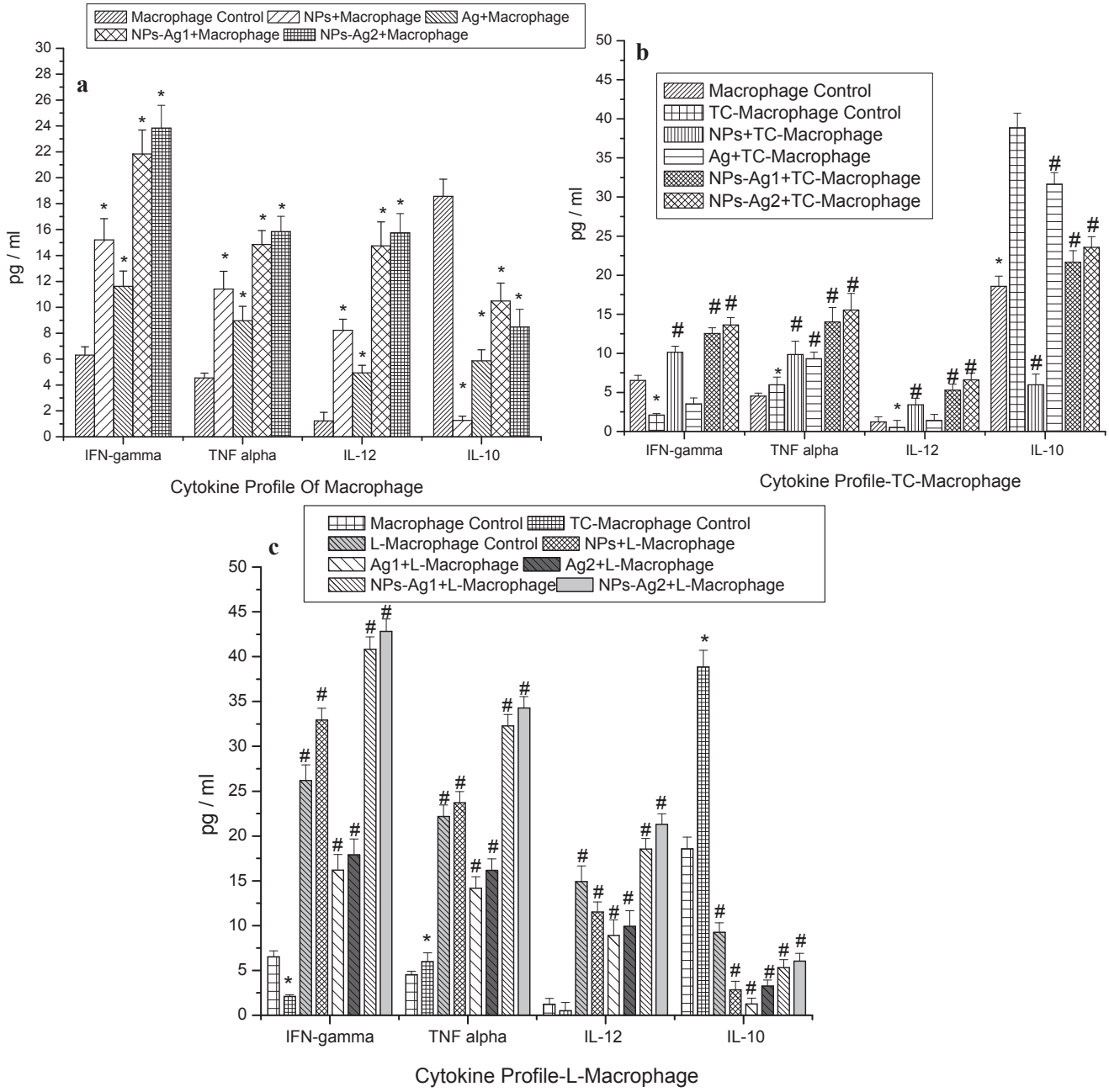

Fig. 2. Alteration of the cytokine profile of normal macrophages (MΦ) (a), tumor conditioned macrophages (TC-MΦ) (b) and LPS stimulated TC-MΦs (c) in response to NPs, Only Ag and NPs-Ag complex. LPS was used as a positive control. Values are expressed as mean ± SEM, * (asterisks) indicates the significant difference as compared with control group. The p values are < 0.05.

incubated in RPMI medium with 5% FCS for 24 h at 37 °C. Pulsed MΦ, TC-MΦ and L-MΦ were added to each well at the ratio of 5:1 or 10:1 (macrophages: cancer cells), and were then incubated for 1, 3 and 5 days at 37 °C. The cancer cell viability was estimated by MTT assay.

2.13. $CD4^+$ T cells proliferation assay

T cells were isolated by using nylon wool coloum from human blood and co-culture with NPs-Ag pulsed MΦ, TC-MΦ and L-MΦ. After treatment schedule, supernatant was isolated and used for cytokine assay. Before to assessing macrophage-CD4 + T cell interactions, we were characterized the CD163 (PE conjugate, Molecular Probes) positive macrophage populations by FACS. Then the isolated lymphocytes were incubated for 30 min at room temperature with fluorescein isothiocyanate (FITC)-conjugated anti-human $CD4^+$ monoclonal antibody. After three washings, samples were resuspended in PBS and analyzed with by flow cytometer (BD FACS). The results were given as the percentage of positively stained cells.

2.14. In vivo survival assay

Swiss mice (age, 6–8 weeks, body weight 25–30 g) will purchase from suppliers. Autoclaved dry pellet diet and water will give *ad libitum*. Maintenance and treatment of animals will give according to the guidelines established by the Institutional Animal Care and Ethics Committee Vidyasagar University.

A 4% of the starch suspension was injected subcutaneously into mice and allowed over night starving. The very next day the peritoneal macrophages (MΦ) were isolated using ice chilled 50 mM PBS (pH-7.0) followed by three times washing with incomplete RPMI media. The

isolated MΦ were divided and treated similar that of Section 2.5 by using mice specific DLA tumor supernatant instead of a human cell line.

Seven groups of Swiss mice (n = 4 in each group) were immunized with unplused MΦ (**Gr. I**), Ag-MΦ (**Gr. II**), Ag-NPs-MΦ (**Gr. III**), TC-MΦ (**Gr. IV**), Ag-NPs-TC-MΦ (**Gr. V**), L-MΦ (**Gr. VI**) and Ag-NPs-L-MΦ (**Gr. VII**) (2×10^5 cells in each case) weekly for three times in total. Three days following completion of the immunization, mice were inoculated with DLA tumor cells obtained from 90 to 95% confluent cultures (1×10^7) intraperitonially [19]. The survival time in terms of percentage of increased life span was measured by the following formula

$$\text{Increase in life span} = (T-C) \times 100$$

where the T = number of days the treated animals survived and C = number of days the control animals survived. We considered 50 days as a cut off for survival time.

2.15. In vivo tumor growth restriction assay

Nine groups of Swiss mice (n = 4 in each group) were immunized with unplused and different pulsed macrophages. Herein, Gr. I- Negative Control, Gr. II- Tumor control, Gr. III- unplused MΦ + Cancer, Gr. IV- Only Ag pulse MΦ + Cancer, Gr. V- NPs-Ag pulse MΦ + Cancer, Gr. VI- TC-MΦ + Cancer, Gr. VII- Ag-NPs pulsed TC-MΦ + Cancer, Gr. VIII- L- MΦ + Cancer and Gr. IX- Ag-NPs pulsed L-MΦ + Cancer. Three days following completion of the immunization, mice were inoculated with Dalton's lymphoma (acetic) cells (DLA) (1×10^7) intraperitoneally. The tumor size was measured, starting from day 0 to day 9, day 17, and day 50 and after day 100. The amount of DLA cells was analyzed by aspirates the peritoneal fluid (Ascetic fluid) followed by spin at 1500 rpm for 5 min. The volume of the DLA cells was used to analysis the tumor volume in milliliters (ml) unit.

2.16. Protein estimation

Protein content was determined using bovine serum albumin as a standard according to the method of Lowry et al. [26].

2.17. Statistical analysis

Each of the above assays was performed in triplicate. The data were expressed as mean ± SEM, n = 6. Comparisons between the means of control and treated group were made by two-way ANOVA test (using a statistical package, Origin 6.1, Northampton, MA 01,060 USA) with multiple comparison *t*-tests, $p < 0.05$ as a limit of significance.

3. Results

3.1. Synthesis and characterization of cobalt oxide nanoparticles

Transmission electron microscopy (TEM) was used to study the morphology and topography of the samples. The results are shown in Fig. 1. The TEM and high-resolution TEM (HRTEM) images (Fig. 2b) show mono disperse nanoparticles with an average diameter of 11.8 nm. The Co signal was detected by EDX of the nanoparticles synthesized by calcinations method as shown in Fig. 1d. HRTEM revels the lattice fringes with the inter-fringe distance 0.21 nm. The grain boundaries oriented in different directions as seen from the figure suggests the polycrystalline nature of the sample. In addition to real-space fringe spacing analysis selected area electron diffraction (SAED) from a large region containing NPs also suggests the lattice spacing of the polycrystallinity of the sample. XRD patterns of cobalt oxide nanoparticle are shown in Fig. 1c. X-ray powder diffraction patterns were taken in reflection mode CuKα (λ = 1.5406 Å) radiation in the 2θ range from 10θ to 90θ on a Panalytical High Resolution XRD). The diffractogram of the CoO NPs (Fig. 1c) shows the presence of peaks at around 2θ 18.75°, 31.04°, 36.86°,44.82°, 59.22°,65.37° corresponding to (1 1 1), (2 2 0), (3 1 1), (4 0 0), (5 1 1) and (4 4 0) plane (JCPDS card no. 80-1533). The dÅ value obtained from SAED gives a similar matching rather than appropriate. Calculated dÅ from SAED − 2.228 Å, 1.82 Å, 1.518 Å, 1.07 Å, 1.138 Å, obtained similar dÅ from JCPDS card no. 80-1533-1.1337 Å (5 5 1), 1.5582 (5 1 1) Å, 1.8576 Å (3 1 1), 2.02 Å (4 4 0). This change is possibly due to the biological impurities used as in sito reducing and coating agent (Fig. 1).

3.2. Effects of tumor cell line conditioned-media on human monocytes

We conditioned monocytes with two different leukemic cell lines supernatant (Jurkat and KG-1A) and noticed that monocytes differentiation was induced in macrophages. Therefore, we decided to restrict our investigation to assess the anticancer activity of the conditioned macrophage on Jurkat and KG-1A cell lines, using homogenous cultures of Jurkat, KG-1A and the normal human macrophage as negative controls. The supernatant from Jurkat and KG-1A induced a strong differentiation of monocytes that became larger, with ruffling membrane typical of macrophages (Fig. S1).

Supplementary data associated with this article can be found, in the online version, at https://doi.org/10.1016/j.cyto.2018.06.035.

3.3. Protein quantification

The successful conjugation of the Ag with the PMIDA-CoO NPs was facilitated by EDC and NHS. EDC and NHS were reacted with the surface carboxylate (−COOH) group on the nanoparticle to yield an O-acyl-isourea active intermediate. This intermediate is then attacked by a primary amine ($-NH_2$) group of the protein's lysine side chain, forming a stable covalent bond between the lysate antigen and the particle. The lysate antigen1 (Ag-1) bound NPs were 64.75% (0.31 mg/ml) and antigen 2 (Ag-2) was 68.35% (0.33 mg/ml) after 24 h (Fig. S2). The antigen concentrations of the stock solutions were adjusted at 0.48 mg/ml. After conjugation, the protein antigen concentrations were estimated and we found that the protein antigen concentrations were less depending on exposure of time (Fig. S3). Protein (CL antigens) release was found to be time dependent. This finding was due to the large concentration gradient between the CL–PMIDA–CoO complex and the outer water phases. The biphasic release pattern is potentially useful for delivery of antigens to macrophages, as it provides a continuous supply of antigens to the macrophages (Fig. S4).

3.4. NPs-Ag induced activation of pro-inflammatory cytokines in TC-MΦ

To better characterize the differentiated cells, we measured the NPs-Ag stimulated release of cytokines by MΦ (Fig. 2a), TC-MΦ (Fig. 2b) and L-MΦ (Fig. 2c) and noticed that NPs-Ag complex induced expression of IFN-γ and TNF-α high amounts. Similarly, LPS produced IFN-γ and TNF-α very high quantity. Notably, MΦ, TC-MΦ and L-MΦ produced IL-12 after NPs-Ag or LPS stimulation (Fig. 3).

3.5. NPs-Ag induced ROS generation activated p38 MAPK in TC-MΦ

Previously we showed that NPs-Ag complex modulate the pro-inflammatory cytokine production by TC-MΦ was executed through activation of ROS and p38MAPK. So, we were eager to check the activation status of the ROS (Fig. 3 and p38MAPKs (Fig. 4) in TC-MΦ following NPs-Ag complex treatment at different hours. The results showed that NPs-Ag complex induced intracellular ROS (Fig. 3a). Our analysis showed that NPs-Ag complex treatment caused phosphorylation of p38MAPK, which peaked at 2 h (4.53%) and remained, elevated up to 3 h (data not shown) in the TC-MΦ (Fig. 4). However, we did not detect any modulation in phosphorylation of ERK1/2 or JNK following NPs-Ag complex treatment. Then we studied the participation of ROS in NPs-Ag complex mediated activation of p38MAPK. We observed that pretreatment of NAC significantly inhibited NPs-Ag complex mediated

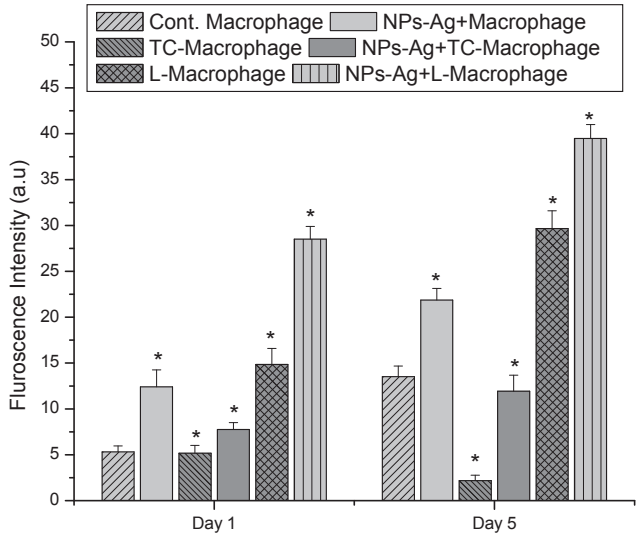

Fig. 3a. Change of a ROS profile of normal macrophages MΦ, tumor conditioned macrophages TC-MΦ in response to NPs-Ag complex. LPS stimulated TC-MΦs were used as a positive control. Values are expressed as mean ± SEM, * (asterisks) indicates the significant difference as compared with control group. The p values are < 0.05.

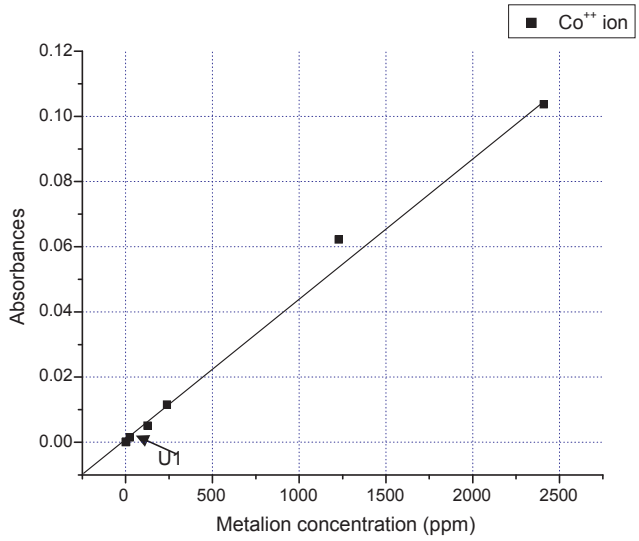

Fig. 3b. Cobalt ion release was measured by atomic absorption spectroscopy, where U1 denotes Co^{++} ion release from 25 μg/ml of NPs-Ag complex.

phosphorylation of p38MAPK in TC-MΦ after 2 h (0.75%) (Figs. 4 and 5a–5d).

3.6. Critical role of NADPH oxidase in ROS production

Studies from different scientific groups strongly suggest that induction of ROS was initiated by the activity of NADPH oxidase [4,33]. A major source of ROS is produced in the mitochondria. Electron leakage from the mitochondrial respiratory chain may react with molecular oxygen, resulting in the formation of superoxide, which can subsequently be converted to other ROS. So, we designed our experiments to investigate whether augmented production of superoxide increased the intracellular ROS level and thus, supported the production of pro-inflammatory cytokines by NPs-Ag pulsed TC-MΦ. We found that before NPs-Ag pulsed NADPH oxidase activity in TC-MΦ were 0.52, 0.61, 0.55 nMol/Min/10^6 Cell on 1–5 h respectively, but the enzyme activity was increased upto 2.32, 9.32, 6.73 nMol/Min/10^6 Cell

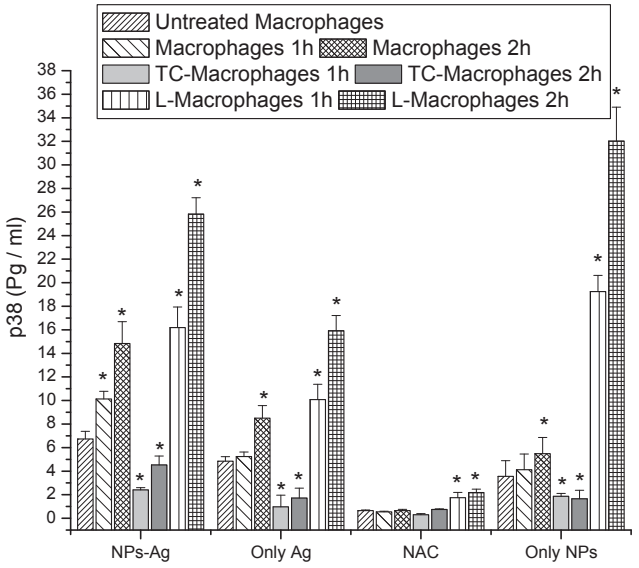

Fig. 4. Activation of p38 MAPK of normal macrophages MΦ, tumor conditioned macrophages TC-MΦ in response to NPs, Only Ag, and NPs-Ag complex after 1 h and 2 h intervals. LPS stimulated TC-MΦs were used as a positive control. Values are expressed as mean ± SEM, * (asterisks) indicates the significant difference as compared with control group. The p values are < 0.05.

(Fig. 6a). It was observed that the enzyme activity was increased at 2 h.

3.7. ROS-induced activation of p38 MAPK critically regulated the cytokine (IFN-γ) production by NPs-Ag complex pulsed TC-MΦ

Earlier studies showed that cell lysate conjugated PMIDA-CoO NPs crucially involved in the uplift of IFN-γ, TNF-α, and IL-12 production by MΦ, TC-MΦ and L-MΦ [8]. Herein, we ascertain the involvement of NPs-Ag complex induced ROS generation in the alteration of IFN-γ profile of tumor conditioned macrophages, we pretreated MΦ, TC-MΦ and L-MΦ with a ROS and p38 MAPK inhibitor, and our based ELISA studies (Fig. 6b) revealed that pretreatment with inhibitors assuaged the effect of Ag-NP complex and LPS in terms of altered IFN-γ level of MΦ, TC-MΦ and L-MΦ. This result aggravated us to further explore the mechanistic details involved in NPs-Ag mediated modulation of the TC-MΦ phenotype.

3.8. Anticancer activity of TC-MΦ

MΦ, TC-MΦ and L-MΦ were co-cultured with Jurkat and KG-1A cells for 1, 3, and 5 days. Decrease in the viability of Jurkat and KG-1A was observed when co-cultured with NPs-Ag pulsed MΦs from the entire group. Figs. 7 and 8 showed the death rate of Jurkat and KG-1A cells with time when co-cultured with pulsed macrophages at the ratio of 5:1 or 10:1 with respect to the negative control. The results are given in terms of percentage of relative viability, which is the percentage of cells that remain viable when compared to a single culture of Jurkat and KG-1A cells. As shown in Fig. 7 during the co-culture of NPs-Ag pulsed TC-MΦ with Jurkat cells at the ratio of 5:1, the percentage of Jurkat cell viability in day 1 was 84.73%, in day 3 was 73.85% and 61.7% on day 5. At the ratio of 10:1 the percentage of cell viability was decreased on day 1, 3 and on day 5 were 74.73%, 63.85% and 52.7% respectively (Fig. 8). The percentage of KG-1A cell viability at 5:1 ratio on day 1 was 86.43%, on day 3 was 78.68% and 66.7% on day 5. At the ratio of 10:1 the percentage of cell viability was decreased on day1, 3, and on day 5 were 78.43%, 69.68%, 66.7% respectively. All the results were significant at p < 0.05 level. Whereas un-pulsed TC-MΦ killed 91.03% Jurkat cells and 92.17% KG-1A cells on day 5 at 10:1 ratio. This cancer cell death was facilitated by the increased cytokines (INF-γ, TNF-

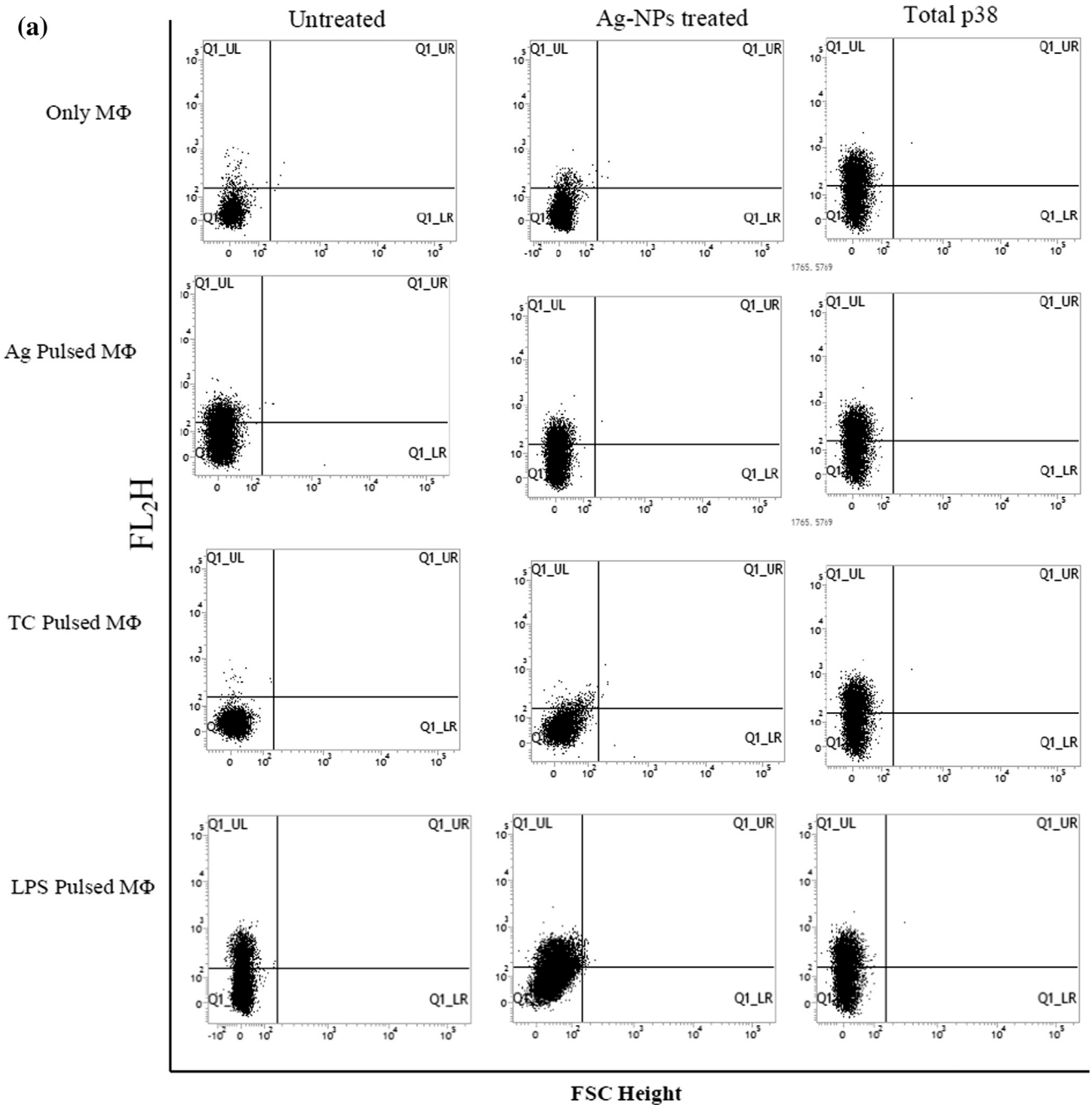

Fig. 5a. Expression of p-p38 MAPK of normal macrophages (MΦ), antigen pulsed macrophages (MΦ), tumor conditioned macrophages (TC-MΦ) and LPS pulsed TC-MΦ in response to NPs-Ag complex, after 1 h was determined by FACS analysis. LPS was used as positive control.

α, and IL-12) (Fig. 3) especially TNF-α, and IL-12. An increase of INF-γ stimulated the production of IL-12 and TNF-α. As the application of TNF-α inhibitor was decrease the cell death. Our previous study postulated that the antigen conjugated nanoparticles induced TNF-α from macrophages and these TNF-α initiates' cancer cell death [9]. From our result (Fig. 3) and our previous study, we may state that the TNF-α induces the death receptor mediated cancer cell death.

3.9. Activation of ROS and p38 MAPK critically regulated the anti-tumorogenic activity NPs-Ag complex pulsed TC-MΦ

Therefore, we asked whether NPs-Ag mediated ROS generation could trigger different MAPKs, essentially modulated the behavior of anti-immunogenic macrophage (M2) toward the pro-immunogenic macrophage (M1). Herein, we used pharmacological inhibitors of p38 MAPK and tried to interpret the role of p38 MAPK on NPs-Ag pulsed TC-MΦ. We observed that of with ROS inhibitor (NAC), TNF-α inhibitor (POF) and p38MAPK inhibitor (PY-MZ) pretreatment TC-MΦ induced cancer cell proliferation even after NPs-Ag pulsation (Fig. 9). Same kinds of results were noted on TNF-α inhibitor pretreated TC-MΦ followed by NPs-Ag pulsation. Thus, p38MAPK activation is involved in NPs-Ag complex-mediated up-regulation of IFN-γ and IL-12 production as well as down-regulation of IL-10 by TAMs was happening (Fig. 9).

3.10. Activation of p38MAPK through NPs-Ag complex mediated increment of IL-12 from TC-MΦ

In the course of our investigation, we checked the production of IL-

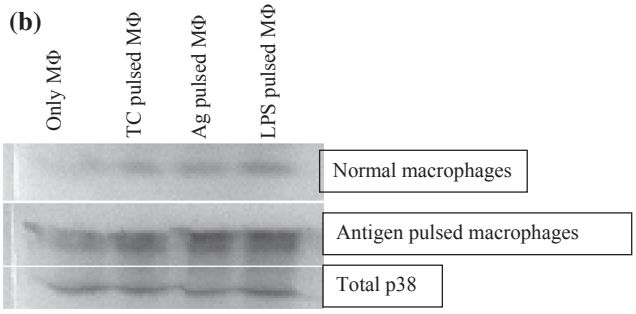

Fig. 5b. Expression of p-p38 MAPK of normal macrophages (MΦ), tumor conditioned macrophages (TC-MΦ), antigen pulsed macrophages (MΦ) and LPS pulsed TC-MΦ in response to NPs-Ag complex, after 1 h was determined by Western blotting analysis. LPS was used as positive control.

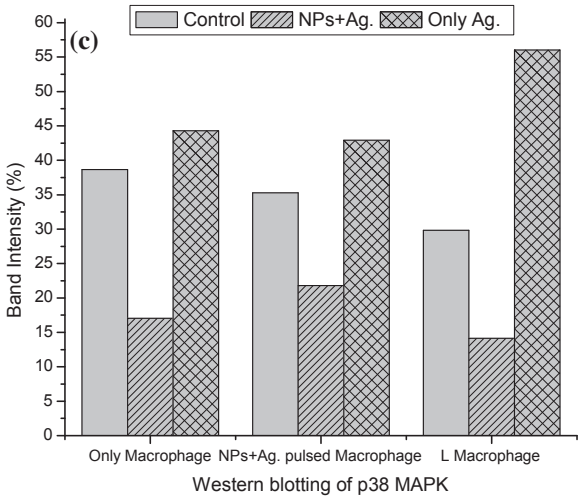

Fig. 5c.

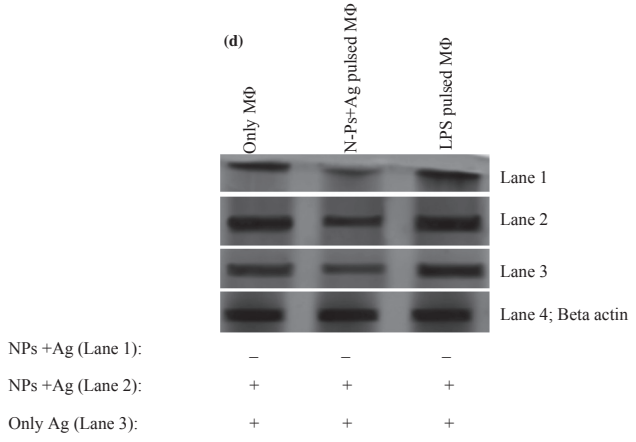

Fig. 5d. Expression of p-p38 MAPK of normal macrophages (MΦ), nano-antigen pulsed macrophages (MΦ) and LPS pulsed TC-MΦ in response to NPs-Ag complex, after 1 h was determined by Western blotting analysis. LPS was used as positive control.

12 by NPs-Ag complex treated TC-MΦ. ELISA data indicated that NPs-Ag complex treatment augmented the IL-12 level in TC-MΦ (Fig. 9). We had shown that NPs-Ag pulse TC-MΦ release higher amount of IFN-γ (Fig. 3) which dictates the simultaneous production of different cytokines, e.g., IL-12 (Fig. 10). The presence of IFN-γ strongly enhanced IL-12 production by human DCs and macrophages [34,21,15]. Other than IFN-γ, activation of p38MAPK strongly enhanced IL-12 production [34,21,15]. Hence, it may suggest that NPs-Ag complex mediated

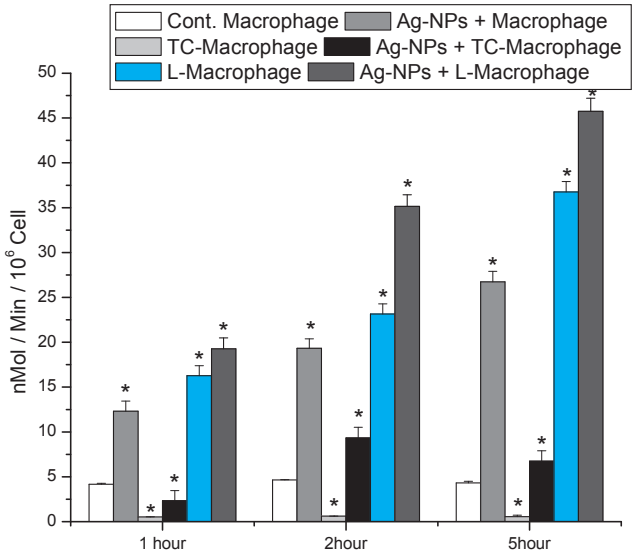

Fig. 6a. Change of a NADPH Oxidase profile of normal macrophages MΦ, tumor conditioned macrophages TC-MΦ in response to NPs-Ag complex. LPS stimulated TC-MΦs were used as a positive control. Values are expressed as mean ± SEM, * (asterisks) indicates the significant difference as compared with control group. The p values are < 0.05.

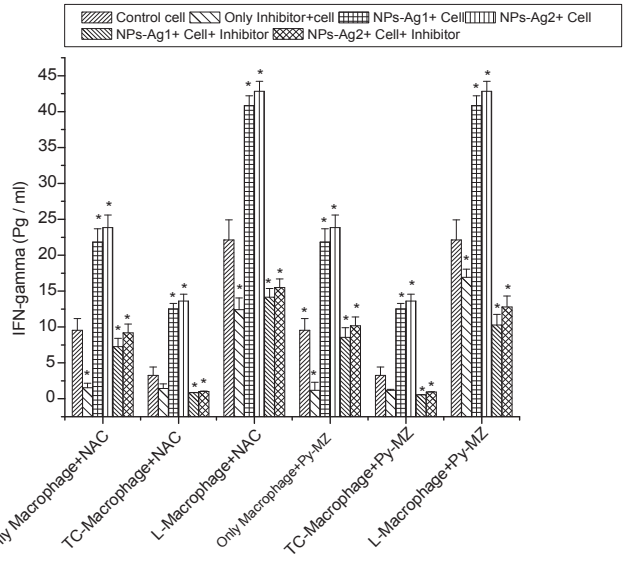

Fig. 6b. The IFN-γ secreted from MΦ, TC-MΦ, L-MΦ was estimated by ELISA in the presences or absences of NPs Ag alone, inhibitors alone and inhibitors + NPs-Ag complex. All the measurements were performed in triplicate. Values are expressed as mean ± SEM, * (asterisks) indicates the significant difference as compared with control group. The p values are < 0.05.

activation of p38MAPK induces the generation of IFN-γ, which in turn, maintains NPs-Ag complex mediated prolonged IL-12 production and down-regulation of IL-10 production by TC-MΦ.

3.11. NPs-Ag pulse TC-MΦ enhanced $CD4^+$ lymphocyte population

The expression of CD163 on TC-MΦ confirmed that tumor supernatant induces M2 phenotype to macrophages up to 9.25% (Fig. 11). NPs-Ag pulsed TC-MΦs were up regulated the $CD4^+$ population. Lymphocyte proliferation was increased in the presences of nanoparticles in culture media. After incubation with NPs-Ag pulsed TC-MΦ for 48 h the percentage of $CD4^+$ cells were increased significantly in NPs pulsed group up to 24% (Fig. 12).

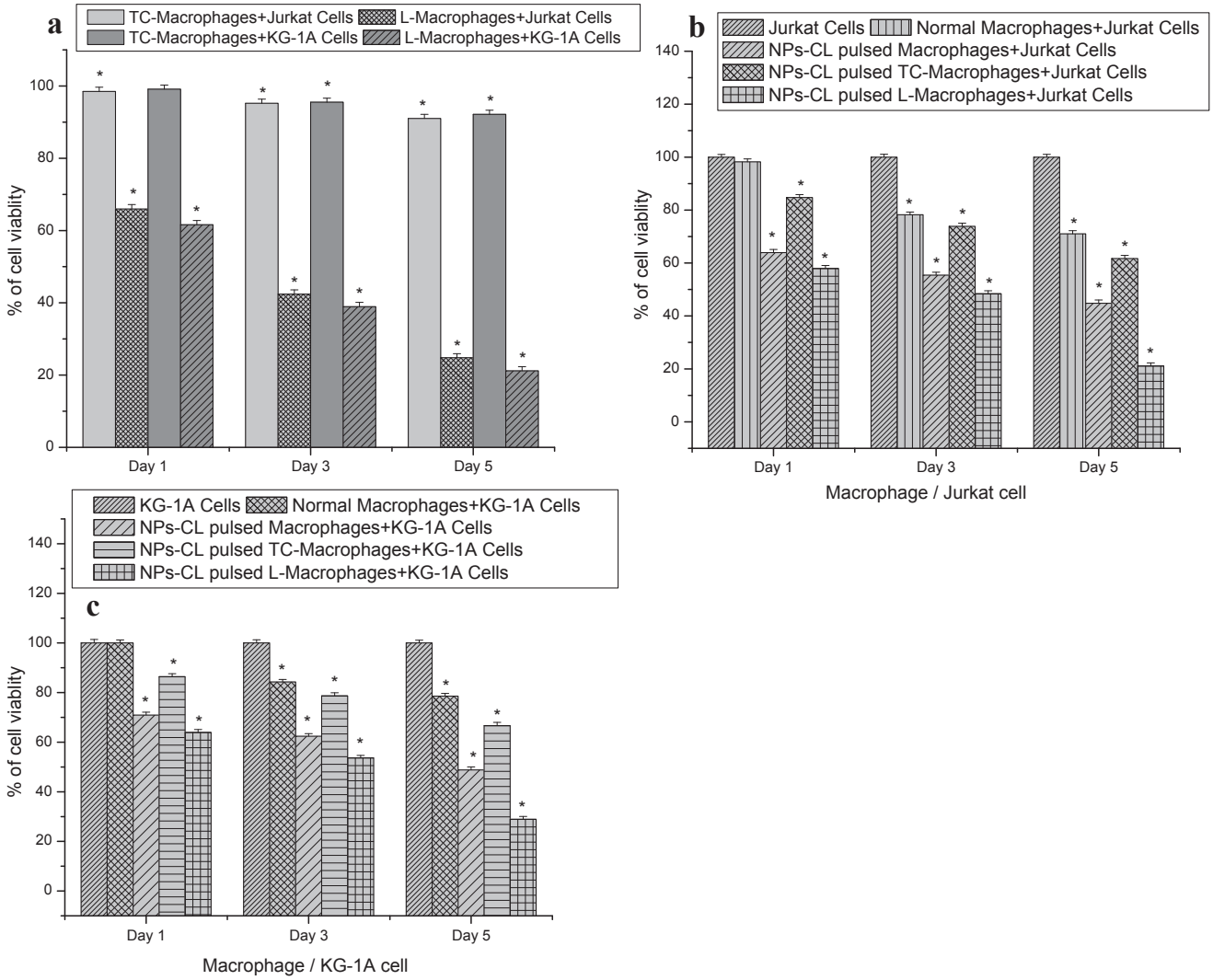

Fig. 7. Cytotoxicity of unplused control MΦ, TC-MΦ, L-MΦ, (a) and NPs-CL (NPs-Ag) pulsed MΦ, TC-MΦ and LPS pulsed TC-MΦ (L-MΦ) co-culture with Jurkat cells (b), and KG-1A cells at 5:1 (c), ratio of macrophage: cancer cells respectively. All the measurements were performed in triplicate. Values are expressed as mean ± SEM, * (asterisks) indicates the significant difference as compared with control group. The p values are < 0.05.

3.12. In vivo survival and tumor growth restriction assay

Administration of NPs-Ag pulsed TC-MΦ (Gr. V) protect from tumor-formation in mice. From the first day of tumor induction we found that the untreated tumor control mice were survived for only 17 days, which was found 46 days in NPs-Ag pulsed-MΦ immunized mice (Gr. -III) and 35 days in NPs-Ag pulsed TC-MΦ immunized mice (Gr. -V) (Fig. 13). Monitoring of tumor growth in all groups of mice clearly demonstrated that tumor growth was restricted in mice immunized with NPs-Ag pulsed TC-MΦ (Fig. 13) in comparison to mice of only Ag pulse MΦ treated groups. Finally, we investigated the efficacy of Ag-NPs pulse macrophages on tumor infected mice. The results showed that the nanocomplex had significantly decreased the volume (14).

4. Discussion

The cancer microenvironment includes innate and adaptive immune cells along with cancer cells. The building of an inflammatory microenvironment endows energy for cancer development and progression [28,43]. Along with the pro-tumorogenic effects, inflammation also influences the host immune response against tumor and can be used in cancer immunotherapy [29].

This study ascertains the paradigm whereby the induction of intracellular ROS by NPs-Ag complex re-induces the cancer microenvironment that markedly reduced cancer cell growth. Herein we disclose that NPs-Ag complex efficiently reprogrammed anti immunogenic TC-MΦ to pro-immunogenic type. Our study shows that NPs-Ag complex mediated ROS generation is the crucial mediator for the activation of p38 MAPK, which in turn modulate the functional phenotype of TC-MΦ towards an effector pro-immunogenic cell. The NPs-Ag complex mediated ROS generation occurs as a result of the presence of Co^{++} ions (Fig. 4). Our previous studies showed that an increasing amount of Co^{++} was augmented excess amount of ROS in PBMCs [10].

Macrophages have appeared as vital therapeutic targets in many diseases. The plastic nature of the macrophage allows re-polarizing anti-immunogenic to pro-immunogenic via production of IFN-γ and IL-12 [37,29]. Studies showed that p38 MAPK is very much essential for macrophage activation of the pro-immunogenic cytokines [27,17]. Existing literature suggests that among the MAPKs, activation of p38MAPK directly regulates IL-12 production by transcriptional interference [27]. This study confirmed that NPs-Ag complex led to a shift the TC-MΦ population anti-immunogenic (M2) to pro-immunogenic (M1) with up-regulation of IFN-γ, IL-12 and TNF-α. Beside this, trim down of IL-10 expression has been shown in NPs-Ag primed TC-MΦ

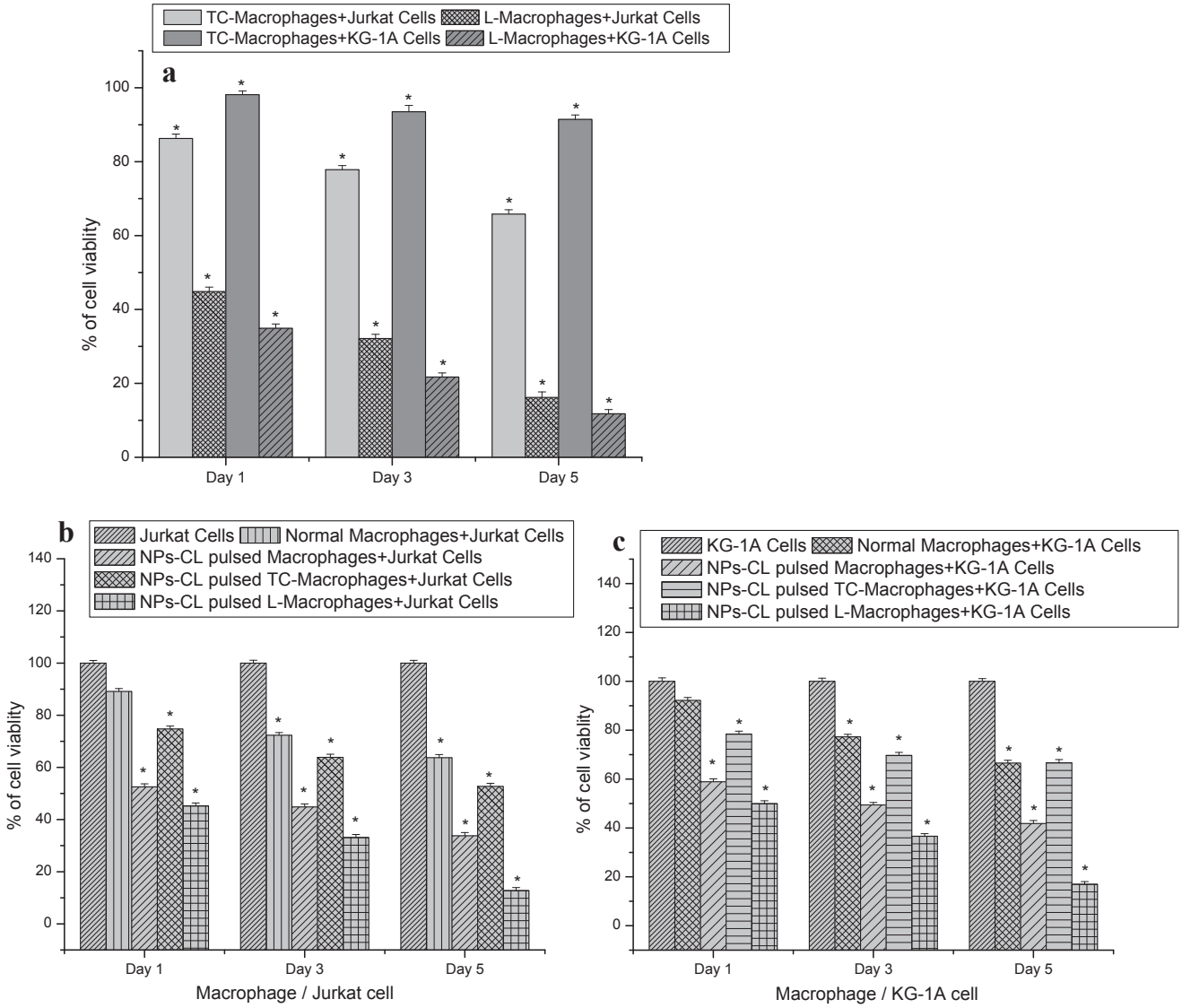

Fig. 8. Cytotoxicity of unplused control MΦ, TC-MΦ, L-MΦ, (a) and NPs-CL (NPs-Ag) pulsed MΦ, TC-MΦ and LPS pulsed TC-MΦ (L-MΦ) co-culture with Jurkat cells (b), and KG-1A cells at 10:1 (c), ratio of macrophage: cancer cells respectively. All the measurements were performed in triplicate. Values are expressed as mean ± SEM, * (asterisks) indicates the significant difference as compared with control group. The p values are < 0.05.

(Fig. 3), results in a re-polarization of M2 like into M1 like macrophages with induction of co-stimulatory molecules. The NPs-Ag complex induced deduction of IL-10 may up-regulates expression of other pro-inflammatory cytokines and has been shown in this study. Down regulation of IL-10 may up-regulated the IFN-γ, MHC-II and co-stimulatory molecules on macrophages followed by activation of Th1 immune response against cancer. The respiratory burst of professional phagocytes activates the NADPH oxidase system, which catalyzes the donation of one electron from NADPH to molecular oxygen, converting it into superoxide anion. The NADPH oxidase system was upregulated by IFN-γ and TNF-α that can influence the NADPH oxidase system an autocrine mechanism [22]. Scientific reports suggested that ROS generated from the NADPH oxidase complex contribute to monocyte/macrophage survival induced by M-CSF via regulation of Akt and p38 MAPK [42]. Our findings suggested that NPs-Ag in TC-MΦ activated NADPH oxidase complex and contribute ROS, which induced activation of p38 MAPK (Figs. 5a and 5b). It is well documented that the generation of ROS leads to the activation of various MAPKs regulating the production of various pro- and anti-inflammatory cytokines in different cell types [7,20,41]. The higher amounts of TNF-α release by NPs-Ag primed phagocytes do not ultimately account for these observations. The most probable explanation is that the NADPH oxidase system in mononuclear phagocytes (Fig. 6a) is activated during its activation by Ag-NPs. These stimuli include not only cytokines but also NADPH oxidase products. The inhibition of ROS production during macrophage differentiation significantly inhibited p38 MAPK activation, implicating a role for ROS as well as MAP kinase in macrophage differentiation. Zang et al. stated that ROS usually associated with the activation and functions of M1 rather than M2 macrophages. In this view, our findings are important for several reasons. First, NPs-Ag mediated ROS production in TC-MΦ reprogrammed them into pro-immunogenic from anti-immunogenic. Second, activation of NADPH Oxidase induces ROS production, which induced activation of p38 MAPK linked to escalate the pro-inflammatory cytokines. Nanomaterials have been shown to modulate expression of cytokines, which are soluble biological protein messengers that regulate the immune system. Stimulated macrophages secreted several cytotoxic factors such as ROS and NO. The hyperactivity of NADPH oxidase elevated ROS, which stimulate the production of TNF-α followed by phosphorylation of p38 MAPK in all set of macrophages. TNF-α, a major mediator of inflammation had played a crucial role in this phenomena.

The NPs-Ag primed TC-MΦ secrete IFN-γ that directly influenced

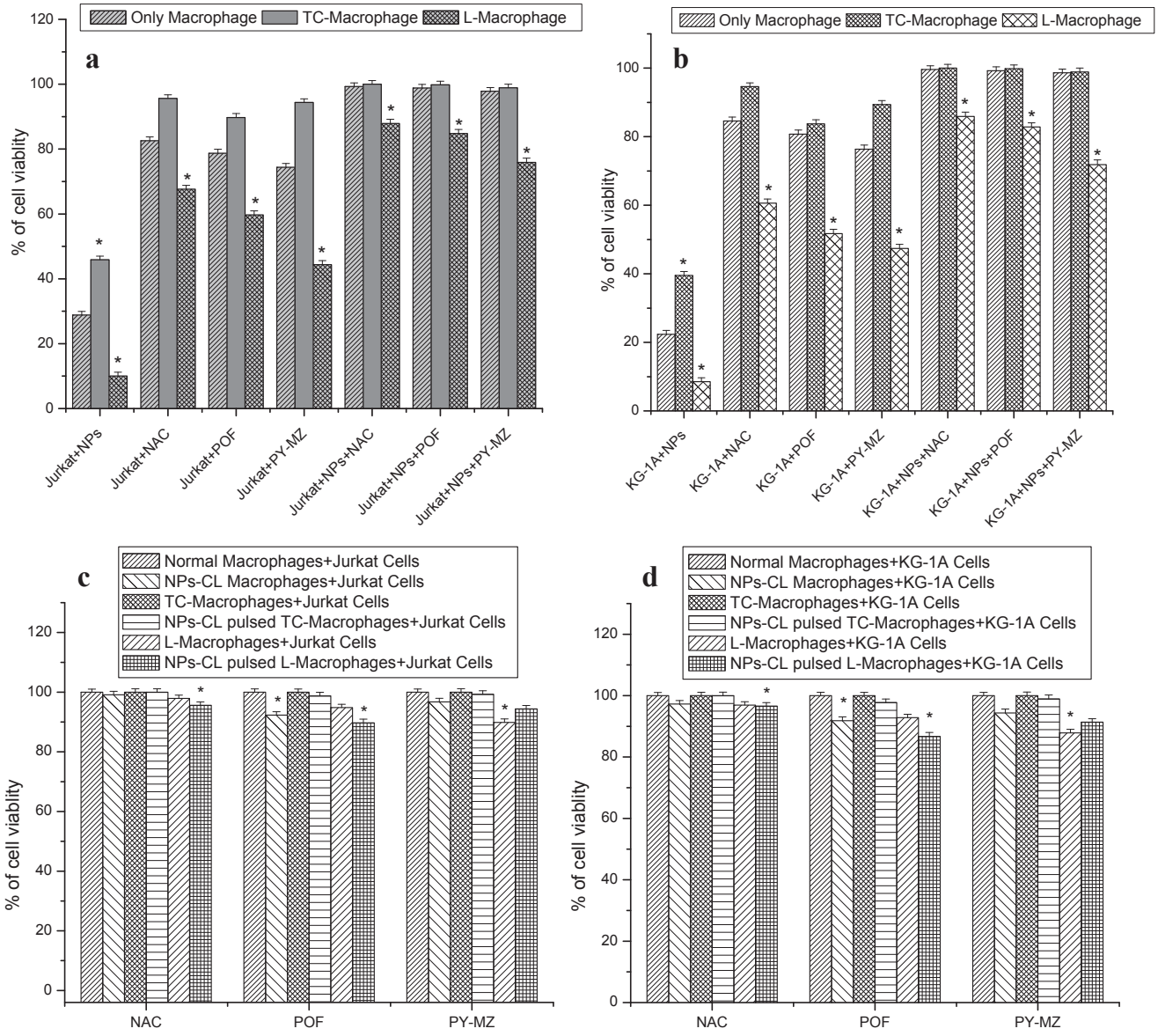

Fig. 9. MΦ, TC-MΦ, L-MΦ, was pretreated with NAC, POF and PY-MZ for 1 h. After incubation, MΦ, TC-MΦ and L-MΦ were incubated with NPs, inhibitors alone and inhibitors with NPs for 24 h. After incubation the pulsed MΦ, TC-MΦ and L-MΦ were co-culture with Jurkat cells (a, c), and KG-1A cells at 10:1 (b, d), ratio and cytotoxicity was estimated by using MTT. All the measurements were performed in triplicate. Values are expressed as mean ± SEM, * (asterisks) indicates the significant difference as compared with control group. The p values are < 0.05.

naive $CD4^+$ cell differentiation toward a Th1 phenotype and enhanced the proliferation of $CD4^+$ T cells two times greater (Fig. 12) which was another key parameter that helps in generation of anticancer immune response. These activated helper T cells were capable of influencing a variety of immune cells for secreting IFN-γ TNF-α, IL-12 cytokines found in our results.

Interaction of NPs-Ag primed TC-MΦ with cancer cell result in a reduction of cancer cell growth. Our study showed that NPs-Ag primed TC-MΦ successfully restricts the *in vitro* (Figs. 7 and 8) and *in vivo* (Fig. 14) tumor growth. The relationship between NPs-Ag primed TC-MΦ with cancer cell may be describe by induction of TNF-α as this cytotoxic factor induces apoptosis/necrosis in cancer cells reported by several scientists. *In vivo* administration of NPs-Ag pulsed macrophage protects from of tumor-formation in mice. From the first day of tumor induction we found that the untreated tumor control mice were survived for only 17 days, which was found 16 days in TC-MΦ immunized mice. Immunization of mice with NPs-Ag pulsed TC-MΦ exhibited better result than the only TC-MΦ in relative to the restriction of the expansion of DL tumor. Our findings indicate that careful titration of Ag-NP-based therapeutic interventions may be successful in elevating a group of cytokines important for eliciting a Th1-mediated immune response with effective anticancer actions. The magnitude of TNF-α induction, as well as other pro-inflammatory cytokines, and their local, regional delivery to tumor sites or other desired areas, will undoubtedly be important parameters when considering PMIDA-CoO NPs for biomedical purposes to achieve the desired therapeutic response without eliciting potential systemic damaging effects from these cytokines. Moreover, our study shows that the synthesized NPs-Ag complex has the capability to polarize M2 type macrophage to M1 type macrophage and this response is shown to be ROS-p38 MAPK-cytokine dependent.

5. Conclusion

The NPs-Ag complex generated ROS-mediated activation of NADPH Oxidase and p38 MAPKs, as well as the alteration of cytokines status, plays an important role in reprogramming of suppressive TC-MΦ

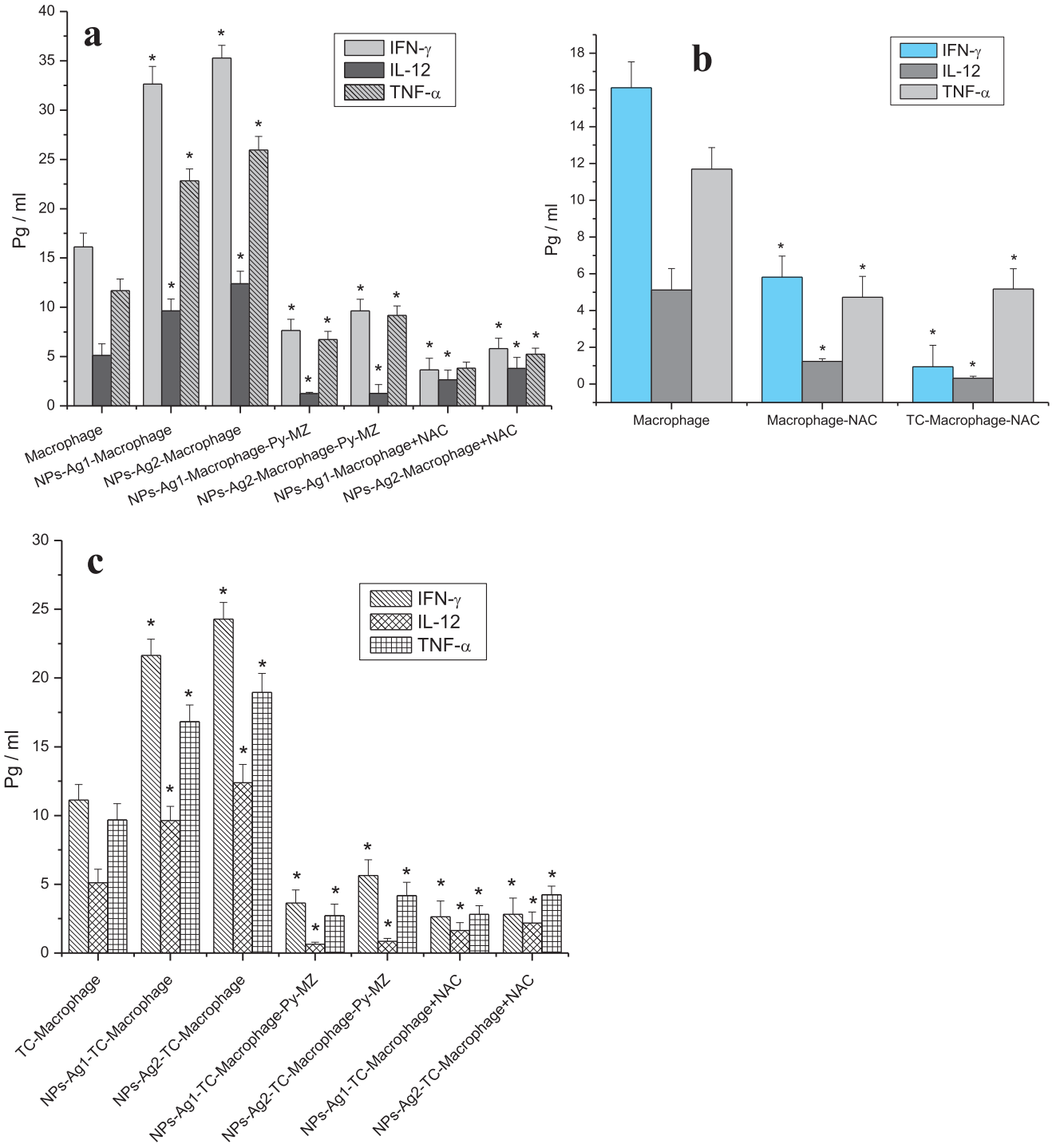

Fig. 10. The IFN-γ, TNF-α, and IL-12 secreted from MΦ (a), TC-MΦ, L-MΦ were estimated by ELISA in the presences or absences of inhibitors pretreated followed by NPs-Ag pulsation at 10:1, ratio. All the measurements were performed in triplicate. Values are expressed as mean ± SEM, * (asterisks) indicates the significant difference as compared with control group. The p values are < 0.05.

toward the pro-immunogenic type. This TC-MΦ can be reprogrammed to promote tumor deterioration through NPs-Ag complex. The NPs-Ag pulsed TC-MΦ efficiently increased IFN-γ and IL-12 which successfully reversed the polarization of anti-immunogenic TC-MΦ to pro-immunogenic TC-MΦ. Generation of ROS in TC-MΦ, showed that they can modulate the NADPH Oxidase and p38MAPK activity and cytokine profile in TC-MΦ. Our study also suggests that although activation of p38MAPK is responsible for IL-12 production by NPs-Ag complex is most vital for reprogramming of suppressive toward the pro-inflammatory type.

Acknowledgement

The authors express gratefulness to Indian Institute of Technology, Kharagpur and Vidyasagar University, Midnapore for providing the facilities to execute these studies.

Conflict of interest

The authors declare that there are no conflicts of interests.

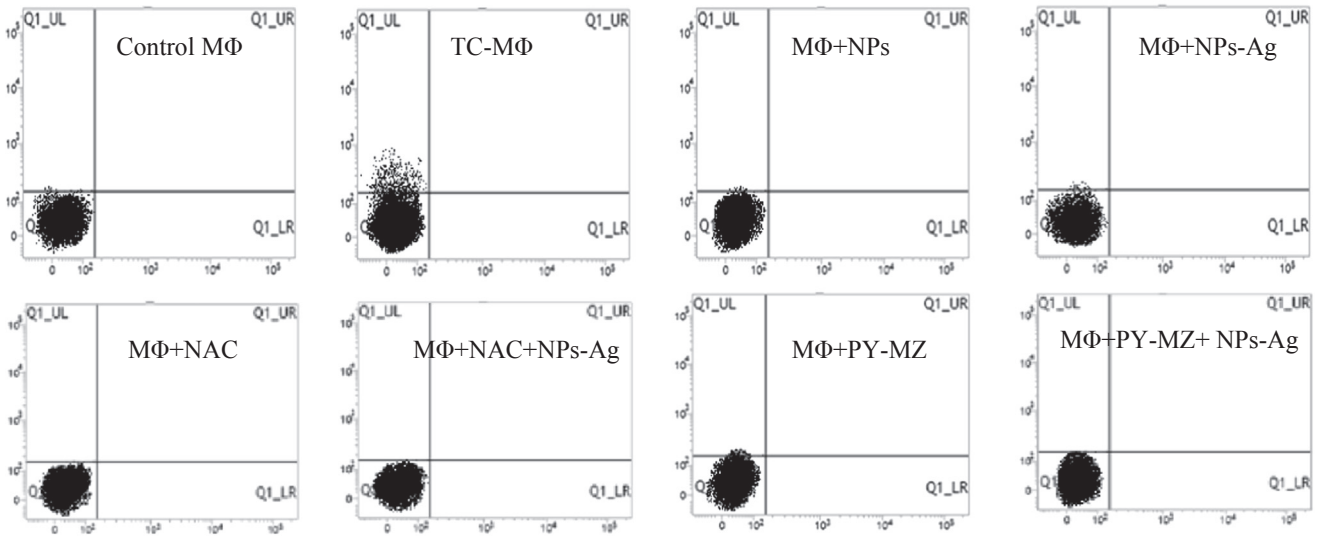

Fig. 11. The expressions of CD163 from MΦs were estimated by FACS in the presences or absences of NAC or PY-MZ pretreated followed by NPs-Ag pulsation at 10:1, ratio. TC-MΦs were used as CD163 positive control.

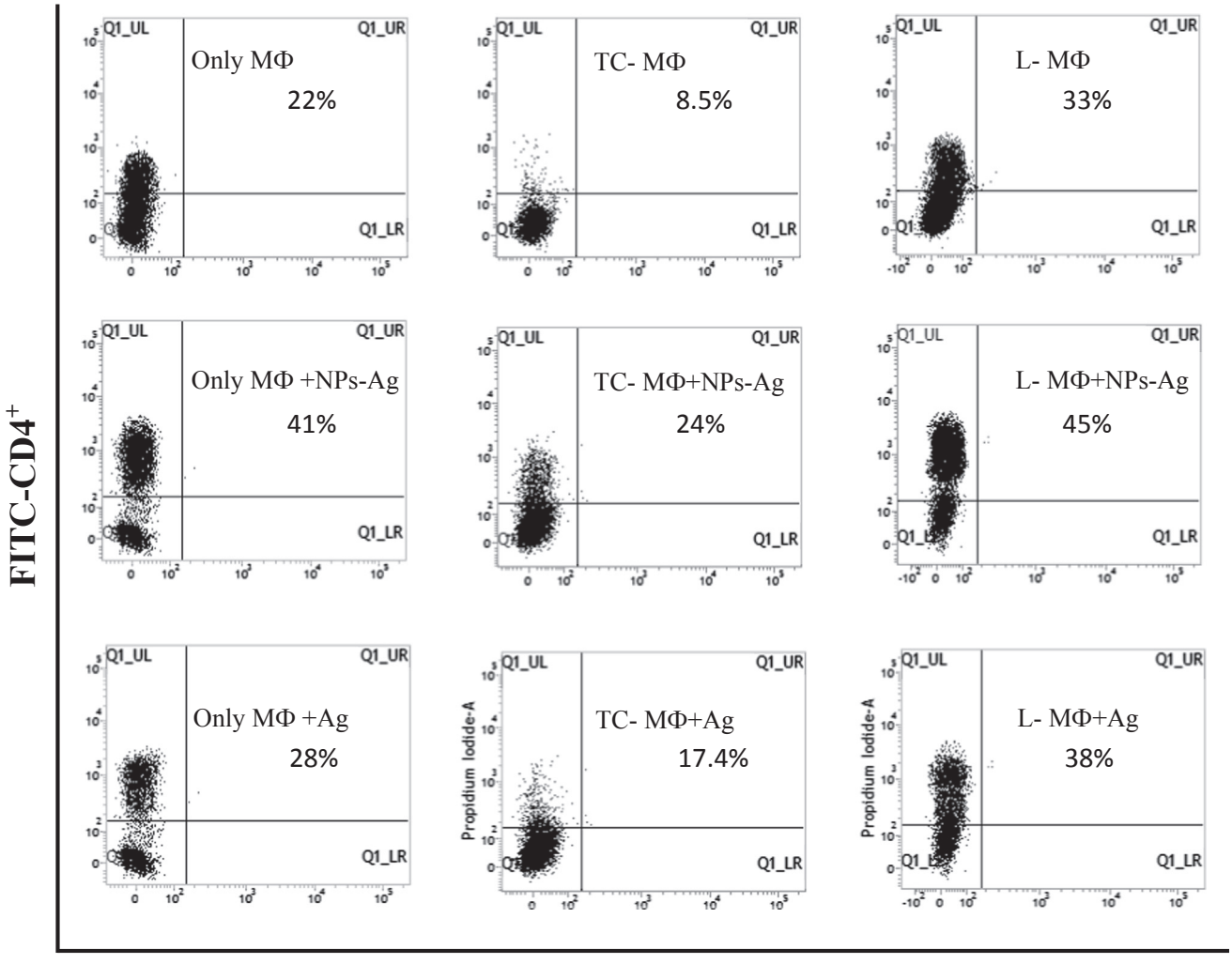

Fig. 12. MΦ, TC-MΦ, L-MΦ, was treated with NPs-Ag and only Ag for 24 h. After incubation the pulsed MΦ, TC-MΦ and L-MΦ were co-culture with T cells for 24 h $CD4^+$ cells were counted by using anti human $CD4^+$ Ab-FITC. The results were expressed as presences of $CD4^+$ cells.

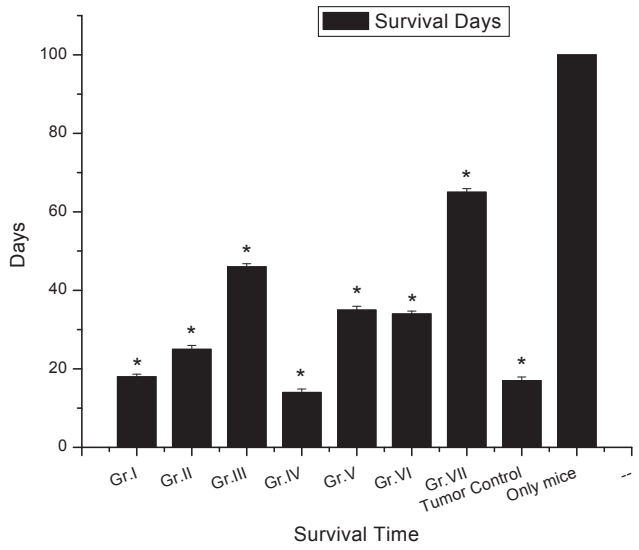

Fig. 13. Survivability and tumor growth restriction of macrophage (Mφ) immunized mice. Mice were immunized with unplused MΦ (Gr. I), Ag-MΦ (Gr. II), Ag-NPs-MΦ (Gr. III), TC-MΦ (Gr. IV), Ag-NPs-TC-MΦ (Gr. V), L-MΦ (Gr. VI) and Ag-NPs-L-MΦ (Gr. VII) weekly for three times in total. Three days following completion of the immunization, mice were inoculated with Dalton's lymphoma (aceytic) cells (DLA) (1×10^7) intraperitoneally. The survival time in terms of percentage of increased life span was measured by using the formula; Increase in life span = $(T - C) \times 100$ (a) and tumor size was measured, starting from day 9 and after every 3 days until day 20. The p values are < 0.05.

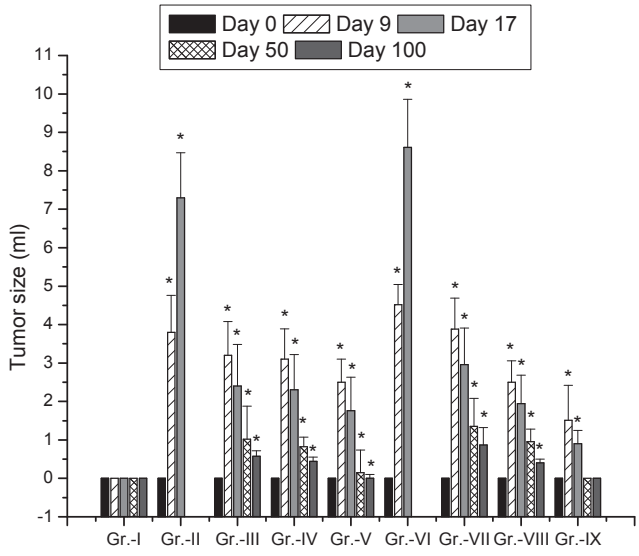

Fig. 14. Tumor growth restriction of macrophage (Mφ) immunized mice. Nine groups of Swiss mice (n = 4 in each group) were immunized with unplused and different pulsed macrophages. Here, Gr. I- Negative Control, Gr. II- Tumor control, Gr. III- unplused MΦ + Cancer, Gr. IV- Only Ag pulse MΦ + Cancer, Gr. V- NPs-Ag pulse MΦ + Cancer, Gr. VI- TC-MΦ + Cancer, Gr. VII- Ag-NPs pulsed TC-MΦ + Cancer, Gr. VIII- L- MΦ + Cancer and Gr. IX- Ag-NPs pulsed L-MΦ + Cancer. Three days following completion of the immunization, mice were inoculated with Dalton's lymphoma (aceytic) cells (DLA) (1×10^7) intraperitoneally. The tumor size was measured, starting from day 0 to day 9, day 17, and day 50 and after day 100. The values are expressed as mean ± SEM. * indicates the significant difference as compared to control group at $p < 0.05$ as the level of significances.

References

[1] J. Banchereau, A.K. Palucka, Dendritic cells as therapeutic vaccines against cancer, Nat. Rev. Immunol. 5 (2005) 296–306.
[2] D.J. Bharali, et al., Novel nanoparticles for the delivery of recombinant hepatitis B vaccine, Nanomedicine 4 (2008) 311–317.
[3] L. Bingle, N.J. Brown, C.E. Lewis, The role of tumour associated macrophages in tumour progression: implications for new anticancer therapies, J. Pathol. 196 (2002) 254–265.
[4] S.K. Biswas, A. Mantovani, Macrophage plasticity and interaction with lymphocyte subsets: cancer as a paradigm, Nat. Immunol. 11 (2010) 889–896.
[5] T. Calzascia, M. Pellegrini, H. Hall, L. Sabbagh, L. Ono, A.R. Elford, T.W. Mak, P.S. Ohashi, TNF-alpha is critical for antitumor but not antiviral T cell immunity in mice, J. Clin. Invest. 117 (2007) 3833–3845.
[6] E.A. Carswell, L.J. Old, R.L. Kassel, An endotoxin-induced serum factor that causes necrosis of tumors, Proc. Natl. Acad. Sci. USA 72 (1975) 3666–3670.
[7] N.S. Chandel, W.C. Trzyna, D.S. McClintock, P.T. Schumacker, Role of oxidants in NF-κB activation and TNF-α gene transcription induced by hypoxia and endotoxin, J. Immunol. 165 (2000) 1013–1021.
[8] S. Chatterjee, A. Mookerjee, J.B. Mookerjee, P. Chakraborty, A. Ganguly, A. Adhikary, D. Mukhopadhyay, S. Ganguli, R. Banerjee, M. Ashraf, J. Biswas, P.K. Das, G. Sa, M. Chatterjee, T. Das, S.K. Choudhuri, A novel copper chelate modulates tumor associated macrophages to promote anti-tumor response of T cells, PLoS One 4 (2009) e7048.
[9] S. Chattopadhyay, S. Dash, T. Ghosh, S. Das, S. Roy, Anticancer and immunostimulatory role of encapsulated tumor antigen containing cobalt oxide nanoparticles, J. Biol. Inorg. Chem. 18 (2013) 957–973.
[10] S. Chattopadhyay, S.K. Dash, S. Tripathy, B. Das, D. Mandal, P. Pramanik, S. Roy, Toxicity of cobalt oxide nanoparticles to normal cells; an *in vitro* and *in vivo* study, Chem. Biol. Interact. 25 (226) (2015) 58–71.
[11] S. Chattopadhyay, S.K. Dash, D. Mandal, B. Das, S. Tripathy, A. Dey, P. Pramanik, S. Roy, Metal based nanoparticles as cancer antigen delivery vehicles for macrophage based antitumor vaccine, Vaccine 10 (2016) 957–967.
[12] C.E. Clark, S.R. Hingorani, R. Mick, C. Combs, D.A. Tuveson, R.H. Vonderheide, Dynamics of the immune reaction to pancreatic cancer from inception to invasion, Cancer Res. 67 (2007) 9518–9527.
[13] C. Domenicotti, B. Marengo, D. Verzola, G. Garibotto, N. Traverso, S. Patriarca, et al., Role of PKC-delta activity in glutathione-depleted neuroblastoma cells, Free Radic. Biol. Med. 35 (2003) 504–516.
[14] Y. Duluc Delneste, F. Tan, M.P. Moles, L. Grimaud, J. Lenoir, L. Preisser, I. Anegon, L. Catala, N. Ifrah, P. Descamps, E. Gamelin, H. Gascan, M. Hebbar, P. Jeannin, Tumor-associated leukemia inhibitory factor and IL-6 skew monocyte differentiation into tumor-associated macrophage-like cells, Blood 110 (2007) 4319–4330.
[15] I.E. Flesch, J.H. Hess, S. Huang, M. Aguet, J. Rothe, H. Bluethmann, S.H. Kaufmann, Early interleukin 12 production by macrophages in response to mycobacterial infection depends on interferon-γ and tumor necrosis factor-α, J. Exp. Med. 181 (1995) 1615–1621.
[16] D.M. Frucht, T. Fukao, C. Bogdan, H. Schindler, J.J. O'Shea, S. Koyasu, IFN-gamma production by antigen-presenting cells: mechanisms emerge, Trends Immunol. 22 (2001) 556–560.
[17] S. Gordon, P.R. Taylor, Monocyte and macrophage heterogeneity, Nat. Rev. Immunol. 5 (2005) 953–964.
[18] S. Gordon, Alternative activation of macrophages, Nat. Rev. Immunol. 3 (2003) 23–35.
[19] S. Goswami, A. Bose, K. Sarkar, S. Roy, T. Chakraborty, U. Sanyal, et al., Neem leaf glycoprotein matures myeloid derived dendritic cells and optimizes anti-tumor T cell functions, Vaccine 28 (2010) 1241–1252.
[20] J. Hamuro, T. Nakazawa, M. Mori, Glutathione redox regulates lipopolysaccharide-induced IL-12 production through p38 mitogen-activated protein kinase activation in human monocytes: role of glutathione redox in IFN-γ priming of IL-12 production, J. Leukoc. Biol. 71 (2002) 339–347.
[21] M.P. Hayes, J. Wang, M.A. Norcross, Regulation of interleukin-12 expression in human monocytes: selective priming by interferon-γ of lipopolysaccharide-inducible p35 and p40 genes, Blood 86 (1995) 646–650.
[22] Y.S. Kim, M.J. Morgan, S. Choksi, Z.G. Liu, TNF-induced activation of the Nox1 NADPH oxidase and its role in the induction of necrotic cell death, Mol. Cell 26 (2007) 675–687.
[23] J.C. Lee, J.T. Laydon, P.C. McDonnell, T.F. Gallagher, S. Kumar, D. Green, D. McNulty, M.J. Blumenthal, J.R. Heys, S.W. Landvatter, J.E. Strickler, M.M. McLaughlin, I.R. Siemens, S.M. Fisher, G.P. Livi, J.R. White, J.L. Adams, P.R. Young, Nature 372 (1994) 739–746.
[24] D. Lison, Boeck M De, V. Verougstraete, M. Kirsch-Volders, Update on the genotoxicity and carcinogenicity of cobalt compounds, Occup. Environ. Med. 58 (2001) 619–625.
[25] M. Look, A. Bandyopadhyay, J.S. Blum, T.M. Fahmy, Application of nanotechnologies for improved immune response against infectious diseases in the developing world, Adv. Drug Deliv. Rev. 62 (2010) 378–393.
[26] O.H. Lowry, N.J. Rosebrough, A.L. Farr, R.J. Randall, Protein measurements with the folin phenol reagents, J. Biol. Chem. 93 (1951) 265–275.
[27] H.T. Lu, D.D. Yangm, M. Wysk, E. Gatti, I. Mellman, R.J. Davis, R.A. Flavell, Defective IL-12 production in mitogen-activated protein (MAP) kinase kinase 3 (Mkk3)-deficient mice, EMBO J. 18 (1999) 1845–1857.
[28] A. Mantovani, P. Allavena, A. Sica, F. Balkwill, Cancer related inflammation, Nature 454 (7203) (2008) 43644.
[29] J.W. Pollard, Trophic macrophages in development and disease, Nat. Rev. Immunol.

9 (4) (2009) 25970.
[30] S. Prasad, V. Cody, J.K. Saucier-Sawyer, W.M. Saltzman, C.T. Sasaki, R.L. Edelson, et al., Polymer nanoparticles containing tumor lysates as antigen delivery vehicles for dendritic cell-based antitumor immunotherapy, Biol. Med. 7 (2011) 1–10.
[31] S.T. Reddy, A.J. van der Vlies, E. Simeoni, V. Angeli, G.J. Randolph, C.P. O'Neil, L.K. Lee, M.A. Swartz, J.A. Hubbell, Exploiting lymphatic transport and complement activation in nanoparticle vaccines, Nat. Biotech. 25 (2007) 1159–1164.
[32] S.T. Reddy, A. Rehor, H.G. Schmoekel, J.A. Hubbell, M.A. Swartz, *In vivo* targeting of dendritic cells in lymph nodes with poly(propylene sulfide) nanoparticles, J. Control Release 112 (2006) 26–34.
[33] J.L. Sardina, G. López-Ruano, L.I. Sánchez-Abarca, J.A. Pérez-Simón, A. Gaztelumendi, C. Trigueros, et al., p22phox-dependent NADPH oxidase activity is required for megakaryocytic differentiation, Cell Death Differ. 17 (2010) 1842–1854.
[34] A. Snijders, C.M.U.T. Hilkens, van der Pouw Kraan, M.M. Engel, L.A. Aarden, M.L. Kapsenberg, Regulation of bioactive IL-12 production in lipopolysaccharide-stimulated human monocytes is determined by the expression of the p35 subunit, J. Immunol. 156 (1996) 1207–1212.
[35] C.M. Solbrig, J.K. Saucier-Sawyer, V. Cody, Polymer nanoparticles for immunotherapy from encapsulated tumor-associated antigens and whole tumor cells, Mol. Pharm. 4 (2007) 47–57.
[36] L. Song, S. Asgharzadeh, J. Salo, K. Engell, H.W. Wu, R. Sposto, T. Ara, A.M. Silverman, Y.A. DeClerck, R.C. Seeger, L.S. Metelitsa, Valpha24-invariant NKT cells mediate antitumor activity via killing of tumor-associated macrophages, J. Clin. Invest. 119 (2009) 1524–1536.
[37] R.D. Stout, S.K. Watkins, J. Suttles, Functional plasticity of macrophages: in situ reprogramming of tumor associated macrophages, J. Leukoc. Biol. 86 (2009) 11059.
[38] R.D. Stout, C. Jiang, B. Matta, I. Tietzel, S.K. Watkins, J. Suttles, Macrophages sequentially change their functional phenotype in response to changes in micro environmental influences, J. Immunol. 175 (2005) 342–349.
[39] R.D. Stout, J. Suttles, Functional plasticity of macrophages: reversible adaptation to changing microenvironments, J. Leukoc. Biol. 76 (2004) 509–513.
[40] C. Sunderkötter, M. Goebeler, K. Schulze-Osthoff, R. Bhardwaj, C. Sorg, Macrophage-derived angiogenesis factors, Pharmacol. Ther. 51 (1991) 195–216.
[41] M. Utsugi, K. Dobashi, Y. Koga, Y. Shimizu, T. Ishizuka, K. Iizuka, J. Hamuro, T. Nakazawa, M. Mori, Glutathione redox regulates lipopolysaccharide-induced IL-12 production through p38 mitogen-activated protein kinase activation in human monocytes: role of glutathione redox in IFN-γ priming of IL-12 production, J. Leukoc. Biol. 71 (2002) 339–347.
[42] Y. Wang, M.M. Zeigler, G.K. Lam, et al., The role of the NADPH oxidase complex, p38 MAPK, and Akt in regulating human monocyte-macrophage survival, Am. J. Respir. Cell Mol. Biol. 36 (2007) 68–77.
[43] L. Zitvogel, L. Apetoh, F. Ghiringhelli, G. Kroemer, Immunological aspects of cancer chemotherapy, Nat. Rev. Immunol. 8 (2008) 5973.